Impact of Postplating Annealing on Defect Activation in Boron-Doped PERC Solar Cells

Benjamin Grübel, Georg Christopher Theil, Sebastian Roder, Tim Niewelt, and Sven Kluska

***Abstract*—In this article, the impact of postplating annealing on the regenerated state of boron-doped p-type passivated emitter and rear cell (PERC) solar cells with plated Ni/Cu/Ag front-side contacts is characterized. The assessment of different plating annealing profiles in the temperature range of 200–300 °C and their impact on light-induced degradation as well as on additional defects are realized by lifetime measurements of nonmetallized solar cell precursors before and after annealing. An observed lifetime degradation indicates that the current process sequence might facilitate bulk defect activation. An alternative process sequence is tested and promising results are presented.**

***Index Terms*—Annealing, light- and elevated-temperature-induced degradation (LeTID), light-induced degradation (LID), passivated emitter and rear cell (PERC) silicon solar cell, plating.**

I. Introduction

PASSIVATED emitter and rear cell (PERC) solar cells with their potential to achieve efficiencies exceeding 24% [1] feature a rising trend in world market share over the last years evolving to be the dominant solar cell concept [2]. In order to advance to solar cell efficiencies of 24% predicted by Min *et al.* [1], the main requirements are technological improvements, such as a reduction of finger width of the front-side metallization. Lately, screen printing achieved finger widths down to 20 μm [3]. The combination of laser contact opening and Ni/Cu/Ag plating is one option to realize a narrow finger width with sufficient finger conductivity and low contact resistances. Furthermore, plating is a lead-free metallization technique that has the potential of cost reduction due to the substitution of most silver with copper [4].

A key aspect in the limitation of PERC solar cells is that light-induced degradation (LID) due to boron oxygen (BO) defects can cause severe losses in the efficiency of the solar cells up to 4–6%$_{\mathrm{relative}}$ under standard test conditions(see [5] and references therein). Although the mechanism is not fully understood, it appears that the losses associated with LID can be reduced to a minimum with the so-called regeneration process [6]. This process enables a stabilization of the metastable defect in an inactive state. However, that state is susceptible to destabilization during thermal treatments, as demonstrated in [7]. They showed the destabilization of the regenerated state of the metastable defect in boron-doped Cz-Si solar cells at temperatures $T > 170$ °C in the dark. Higher temperatures lead to faster destabilization and thereby higher loss of efficiency. Furthermore, Cz-Si has recently been demonstrated to be susceptible to light- and elevated-temperature-induced degradation (LeTID) after PERC process sequences [8]–[10]. LeTID is largely impacted by thermal treatments and can be activated by annealing in the dark [8]. Therefore, plating treatments could activate LeTID, as well.

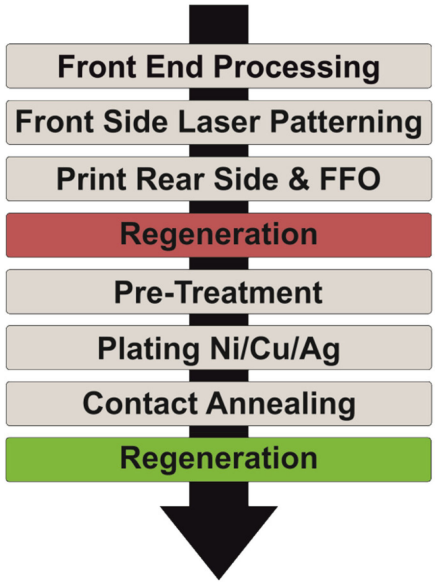

Fig. 1. Standard (red) and developed (green) plating process sequence for front-side metallization of PERC solar cells at Fraunhofer ISE.

The plating sequence for front-side metallization developed at Fraunhofer ISE is displayed in Fig. 1, moving the regeneration process (red) to the end position (green) of the sequence. It involves thermal postplating annealing in order to enhance contact resistance and contact adhesion [11]. Application of this process sequence could be detrimental to the stabilized state of BO defects and could also activate LeTID.

Manuscript received July 26, 2019; revised October 29, 2019 and January 10, 2020; accepted January 16, 2020. Date of publication February 4, 2020; date of current version February 19, 2020. This work was supported by the German Federal Ministry for Economic Affairs and Energy within the Projects "GENESIS" (0324274C) and "TALER" (03EE1021B). *(Corresponding author: Benjamin Grübel.)*

B. Grübel, G. C. Theil, S. Roder, and S. Kluska are with the Fraunhofer Institute for Solar Energy Systems, 79110 Freiburg, Germany (e-mail: benjamin.gruebel@ise.fraunhofer.de; georg.christopher.theil@ise.fraunhofer.de; sebastian.roder@ise.fraunhofer.de; sven.kluska@ise.fraunhofer.de).

T. Niewelt is with the Fraunhofer Institute for Solar Energy Systems, 79110 Freiburg, Germany, and also with the Laboratory for Photovoltaic Energy Conversion, INATECH, University of Freiburg, 79110 Freiburg, Germany (e-mail: tim.niewelt@ise.fraunhofer.de).

Color versions of one or more of the figures in this article are available online at https://ieeexplore.ieee.org.

Digital Object Identifier 10.1109/JPHOTOV.2020.2968110

In this article, we investigate the impact of postplating annealing processes on regenerated PERC solar cells. Furthermore, we will suggest alternatives to the standard plating sequence in order to combine it with the regeneration step [see Fig. 1 (green)].

II. Experiment

Commercial p-type Cz-Si PERC solar cell precursors of 1–2 Ω·cm after front- and rear-surface passivation/before metallization were used to analyze the impact of dark annealing processes on LID. The samples featured a textured front side, a phosphorous emitter, silicon nitride plasma-enhanced chemical vapor deposition (PECVD) antireflection coating and passivated rear side. In order to investigate the impact of the postplating annealing on regenerated p-type PERC solar cells, a process sequence as introduced in Fig. 1 (red) was applied. All samples received a rapid thermal annealing firing treatment at a set peak temperature of 810 °C and a belt speed of 6 m/min using an industrial conveyer belt furnace (RFS 250 Plus, Rehm). The 156 × 156 mm solar cell precursors were subsequently sawn into four equally sized square quarters (∼78 mm × 78 mm). These samples were then exposed to constant low-intensity halogen lamp illumination for 42 h at room temperature to transfer all BO defects to a well-defined degraded state. Then, a regeneration step was performed on a hotplate for 3 h at 140 °C under 0.5–0.7 sun equivalents halogen lamp illumination and ambient atmosphere. The subsequent annealing treatment mimicking contact annealing was varied in annealing temperature and duration. In order to illustrate the potential of complete destabilization of the samples, typical postplating annealing at temperatures between 200 and 300 °C was realized by extending annealing time of usual 1 to 20 min to a maximum value of 300 min. The annealing was performed on a hotplate in the dark in order to avoid occurrence of regeneration and thereby investigate a worst case scenario. After annealing, the samples were exposed to halogen lamp illumination at room temperature to transfer potentially destabilized defects to the recombination-active state.

Charge carrier lifetime measurements were performed at sample temperature of 25 °C and evaluated at an injection level of $1{\cdot}10^{15}$ cm^{-3} using a WCT-120 lifetime tester from Sinton Instruments [12]. As lifetimes were expected below 200 μs, the quasi-steady-state measurement method was applied using a long time constant of the flash lamp [13]. An intrinsic carrier concentration of $n_i = 9.7{\cdot}10^9$ cm^{-3} was assumed for the analysis and implied open-circuit voltages i$V_{\rm oc}$ were determined as well [14]. To demonstrate successful transfer of BO defects in the samples to regenerated state, lifetime measurement were performed before and after regeneration. During plating, a maximum sample temperature of 50 °C is reached. Therefore, it is assumed that this process has negligible impact on the samples, and for experimental simplicity, the plating process and the preceding front-side laser patterning were skipped in the experiment, as indicated in Fig. 2.

A validation of the results on the unmetallized samples is performed in a second step by realizing functional solar cells. Therefore, commercial p-type Cz-Si PERC solar cell precursors after rear-side metallization from a different supplier were used.

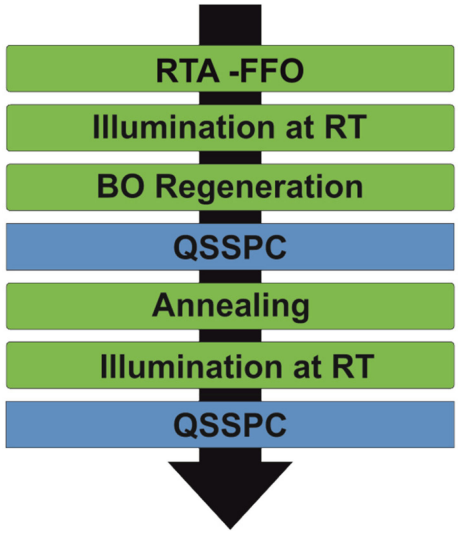

Fig. 2. Process scheme of the performed experiment with process steps (green) and characterization steps (blue).

These precursors featured a textured front side, a phosphorous emitter, silicon nitride PECVD antireflection coating, and full-area screen-printed aluminum rear side. Before rear-side contact firing, the front-side laser patterning (5 BB, 114 Fingers) was performed with an UV-ps laser followed by an industrial firing and regeneration process of the precursor supplier. After that the plating process was performed, as displayed in Fig. 1, by light-induced plating, combining light and carrier injection, followed by a similar variation of annealing temperatures (200–250 °C) and limited annealing times (0–4.5 min) realized in an inline furnace under nitrogen gas atmosphere. The finished solar cells were then degraded and regenerated under the very same conditions as the previous samples. Standard *IV* characterization was realized after degradation and after regeneration.

III. Results and Discussion

A. Dark-Annealing-Induced Degradation

The impact of the annealing process in the dark was analyzed concerning its influence on the stability of the regenerated PERC solar cells. The results for the normalized defect concentration $N(t) = 1/\tau(t) - 1/\tau_{\rm Regenerated}$, with $\tau(t)$ being the measured lifetime at time t and $\tau_{\rm Regenerated}$ the initial lifetime after regeneration, are displayed in Fig. 3 (left). A corresponding evaluation of the $iV_{\rm oc}$ − loss from the same measurements is shown in Fig. 3(right), with $\Delta iV_{\rm oc} = iV_{\rm oc,annealed} - iV_{\rm oc,Regenerated}$, in order to ease comparison of the lifetime sample experiment with the cell results in the succeeding section (see Section III-B).

For all temperatures, an increasing defect concentration as well as an increasing $\Delta iV_{\rm oc}$ − loss can be observed for increasing annealing durations within 10 min. For annealing above 10 min, the defect concentration as well as the $\Delta iV_{\rm oc}$ − loss is further increasing for temperatures of 200–250 °C. However, at 300 °C, the defect concentration and the $\Delta iV_{\rm oc}$ − loss saturate after 10 min. The data points after 100 min suggest a slight recovery. For temperatures below 300 °C, the same trend of the

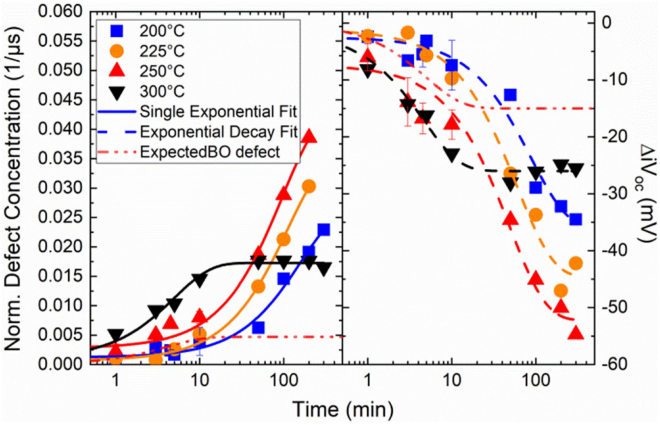

Fig. 3. Normalized defect concentration (left) and decay curves of iV_{oc} destabilization (right) recorded after subsequent annealing degradation of non-metallized samples in the dark. The lines are single exponential fits (left) and exponential decay fits (right). The dash-and-dot line describes the defect concentration and ΔiV_{oc} loss that can be attributed to BO defects at 250 °C (error bars only in the case of multiple samples).

defect concentration and ΔiV_{oc} − loss is presented by Wilking *et al.* [15] and Herguth *et al.* [7], [16], respectively. The trend of the defect concentration and the ΔiV_{oc} − loss was fitted with a single exponential function and an exponential decay fit, respectively. The BO-defect-related defect concentration and ΔiV_{oc} − loss determined by measurements before and after regeneration process is 0.005 $\mu s^{-1} \pm 0.001$ μs^{-1} and 9.7 mV ± 1.3 mV, respectively. The dash-dotted red line in Fig. 3 illustrates the expected effect of BO defect destabilization for the experiment at 250 °C. It was calculated using the time constant reported by Wilking *et al.* [15] for 245 °C combined with the BO defect impact in our samples as extracted from measurements before and after regeneration treatment. Clearly, the observed degradation during dark annealing surmounts the expected defect concentration and ΔiV_{oc} − loss attributed to BO defects revealing the presence of additional defects activated by the annealing process. We observe that the degradation amount exceeding the expected BO defect reactivation follows an exponential behavior with a longer timescale than BO defect reactivation. Determining an activation energy E_A according to a single exponential fit of the measured data lead to an activation energy of $E_A = 0.26 \pm 0.05$ eV. According to the literature reviewed by Niewelt *et al.*, activation energies for the destabilization reaction of 1 eV and above have been reported [6]. This suggests additional defect activation with different activation energies for the samples presented in this article. Unfortunately, our dataset is too limited to extract expressive data, such as additional activation energies, but the trend agrees with what could be expected for LeTID activation [17]. Another aspect supporting the attribution of these defects to LeTID is the indication of a subsequent recovery upon prolonged annealing, as indicated by the 300 °C curve. Independent of the origin or the exact interaction of the defects, our experiment confirms that postplating annealing can have an impact on stabilized PERC solar cells. The specific processing conditions can thereby affect the final efficiency of plated solar cells beyond contact properties.

In the following sections, this article will focus on V_{oc} of solar cells due to experimental reasons. The experiment presented above has, however, demonstrated that we can expect to observe the effects on the cell level. Typical postplating annealing at Fraunhofer ISE are done with temperatures up to 250 °C and maximum duration of 20 min, leading to a maximum loss of 25 mV at 250 °C, as shown in Fig. 3. Even at moderate temperature of 200 °C, a loss of 2–10 mV occurs. It has been taken into account that the fitted curves of the results feature a maximum measurement error of 8 mV. If a certain postplating annealing is required, one must be aware of the considerable loss that V_{oc} will suffer from. Furthermore, postplating annealing even above 250 °C would presumably lead to an even stronger iV_{oc} − loss.

At this point, it can be noted that independent from the exact metallization process, implementing the solar cells in modules implies applying interconnectors and encapsulation requiring elevated temperature processes. Currently lead-containing soldering is the standard process [2] realized at temperature exceeding 220 °C [18] within seconds and additional ramping steps at around 150 °C for few minutes. Encapsulation and lamination of solar cells is typically performed at 150 °C for 7.5–15 min [19]. Therefore, stabilized solar cells might also be susceptible to theses manufacturing processes in terms of defect degradation.

Since any loss in the electrical parameters of a solar cell is undesired, the results of this experiment suggest three mitigation strategies. The first obvious option is to omit the postplating anneal step to avoid affecting the reached BO defect state and possible other defects. The second option is to reduce the annealing duration and temperature to a minimum to reduce ΔiV_{oc} − loss. Both options would constrain or at least limit the beneficial effects of the postplating anneal step on the plates contacts. The third is to avoid the destabilization. Therefore, the regeneration of the solar cells can be either performed after the annealing step [Fig. 1(green)] or—preferably—even simultaneously with it. Using laser-based ultrafast regeneration UFR process enables the regeneration of BO defects above 95% in less than 10 s [20], [21]. Roder *et al.* demonstrated improvement in contact resistance at a temperature of 250 °C within 10 s during the regeneration process [22]. These approaches would not lead to further process steps in the sequence combining the benefits of the postplating anneal step with the regeneration process.

B. Compatibility of Postplating Anneal With Light-Induced Degradation

In order to evaluate whether a regeneration process after the postplating anneal can mitigate LID, we produced fully functional PERC solar cells, as presented in Section II. The results are presented in Fig. 4. The V_{oc} results of the cells are shown after the degradation and after the regeneration process. The *black* data points indicate the reference V_{oc}-value of the plating process without anneal step. At 200 °C, ΔiV_{oc} − loss of 2–3 mV can be observed for a 3-min anneal, whereas the loss increases up to 10 mV for an increased annealing temperature of 250 °C. Furthermore, the extension of the anneal time at 225 °C increases the V_{oc}-loss as well. The results show similar behavior, as already shown in Fig. 3. Subsequently, a regeneration process

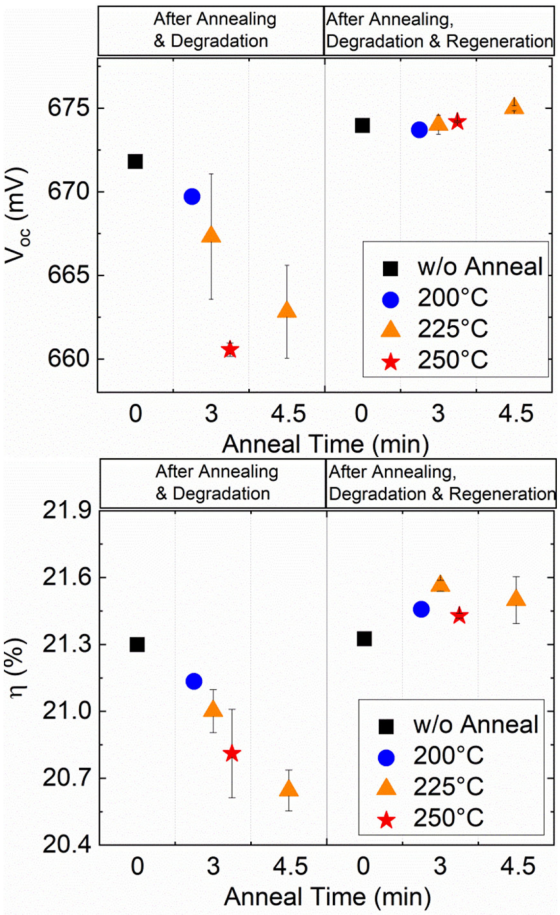

Fig. 4. V_{oc} (top) and η (bottom) of a variation of anneal temperature, a duration after annealing and degradation and after annealing, degradation, and regeneration process (error bars only in the case of multiple samples).

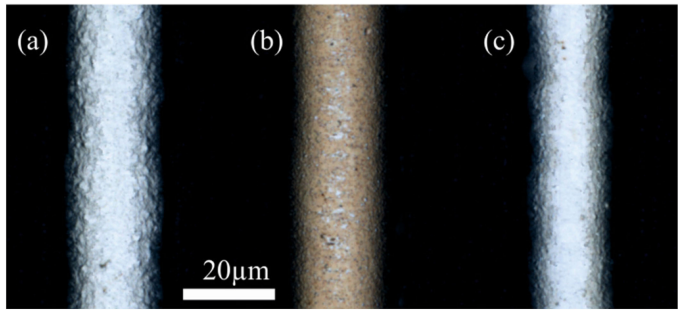

Fig. 5. Images of a plated finger directly after plating (a), after the regeneration process (b), and after a dip in 10% MSA (c) taken with a laser microscope.

was applied on the very same solar cells. At this point, it must be noted that since the regeneration process was performed at ambient atmosphere, the metallization suffered from a corrosion effect (see Section III-C). Nevertheless, as shown in Fig. 4, the initial ΔiV_{oc} – loss was successfully recovered, and the exact same behavior can be observed in the efficiency of the solar cells [see Fig. 4 (bottom)], revealing the feasibility of that process sequence. The occurring variation of the efficiency after the regeneration process originates from variation in J_{sc} and R_s.

C. Discolouration of Metallized Contacts Due to Ambient Atmosphere Annealing

As already observed in the previous section, metals, such as silver and copper, tend to be vulnerable to corrosion, leading to a visible color change at the surface. This effect is widely known for these metals and has been studied in detail in the past [23], [24]. The effect of corrosion is usually associated with the presence of chloride and sulfur under atmospheric conditions [24]. The appearance of the corrosion is also depending on the relative humidity.

In order to characterize the discolouration of the metallization of the solar cells, an optical characterization of the metallized solar cells was performed with a laser microscope. In Fig. 5(a), a plated finger with silver capping directly after plating is displayed. This cell was then regenerated on a hotplate at ambient atmosphere at 140 °C for 180 min, leading to a color change of the finger defined as corrosion visible in Fig. 5(b). Following this, the solar cell was dipped in 10% methansulfonic acid (MSA) resulting in a complete removal of the corroded surface and fully cleaned metallization [see Fig. 5(c)]. It must be pointed out that, *IV* measurements were performed after each process step shown in Fig. 5, showing no clear impact of the discolouration or of the chemical cleaning. Thus, the corrosion of the metallized contacts of solar cells has only an aesthetically impact that can be easily removed. It can be noted that the use of an inert atmosphere avoids the corrosion effect as all solar cells that were annealed after plating under nitrogen atmosphere showed no discoloration.

IV. Conclusion

We demonstrated the critical impact of postplating annealing on lifetime and V_{oc} behavior of stabilized PERC solar cells. Even for low contact annealing temperatures of 200 °C and short annealing durations of 3 min, a significant defect concentration and a degradation of the iV_{oc} of cell precursors and V_{oc} of finished solar cells of 2–10 mV was observed. The loss becomes even more important when the annealing temperature or duration is increased. The origin of the degradation appears to be a combination of multiple defects. A reasonable second defect besides BO defects might be LeTID, which is known to affect Cz monocrystalline p-type solar cells. A detailed investigation of the occurring defects was beyond the scope of this article.

The observed destabilization due to postplating annealing makes it no viable option to perform the regeneration before postplating annealing. Therefore, an alternative process sequence with a regeneration treatment *after* postplating annealing is presented. This process sequence allows to fully avoid annealing-induced losses. Furthermore, the impact of postplating annealing-induced defect losses requires regeneration of plated PERC solar cells after annealing and before *IV* measurement to estimate the full cell efficiency potential.

Depending on the temperature, duration, and atmosphere of the regeneration, discoloring of the plated metal contacts can appear. This corrosion effect is identified as solely aesthetical

issue. Discoloring effects can be avoided by lowering either temperature and/or duration of the regeneration process compared with the lab-type process used in this article or by performing the regeneration under an inert atmosphere. If discoloring cannot be avoided, it can be easily removed by a short chemical dip. Moreover, the application of laser-based regeneration processes could allow a simultaneous regeneration and anneal. One of such processes is the ultrafast regeneration process UFR that could even be performed under controlled atmosphere, while still being compatible with an inline production line.

REFERENCES

[1] B. Min *et al.*, "A roadmap toward 24% efficient PERC solar cells in industrial mass production," *IEEE J. Photovolt.*, vol. 7, no. 6, pp. 1541–1550, Nov. 2017.

[2] International technology roadmap for Photovoltaics, "International technology roadmap for Photovoltaics (ITRPV) 10th ed.," ITRPV, 2019.

[3] F. Clement *et al.*, "'Project Finale' - Screen and screen printing process development for ultra-fine-line contacts below 20µm finger width," in *Proc. 36th Eur. Photovolt. Sol. Energy Conf. Exhib.*, 2019, pp. 255–258.

[4] A. Lennon, J. Colwell, and K. P. Rodbell, "Challenges facing copper-plated metallisation for silicon photovoltaics: Insights from integrated circuit technology development," *Prog. Photovolt.*, vol. 27, pp. 67–97, 2019.

[5] B. Hallam *et al.*, "Eliminating light-induced degradation in commercial p-type czochralski silicon solar cells," *Appl. Sci.*, vol. 8, no. 1, 2018.

[6] T. Niewelt, J. Schon, W. Warta, S. W. Glunz, and M. C. Schubert, "Degradation of crystalline silicon due to boron–oxygen defects," *IEEE J. Photovolt.*, vol. 7, no. 1, pp. 383–398, Jan. 2017.

[7] A. Herguth and G. Hahn, "Kinetics of the boron-oxygen related defect in theory and experiment," *J. Appl. Phys.*, vol. 108, no. 11, 2010, Art. no. 114509.

[8] Daniel Chen *et al.*, "Evidence of an identical firing-activated carrier-induced defect in monocrystalline and multicrystalline silicon," *Sol. Energy Mater. Sol. Cells*, vol. 172, pp. 293–300, 2017.

[9] F. Fertig *et al.*, "Mass production of p-type Cz silicon solar cells approaching average stable conversion efficiencies of 22%," in *Proc. 7th Int. Conf. Silicon Photovolt.*, 2017, pp. 338–345.

[10] K. Ramspeck *et al.*, "Light induced degradation of rear passivated mc-Si solar cells," in *Proc. Eur. Photovolt. Sol. Energy Conf. Exhib.*, 2012, pp. 861–865.

[11] A. Mondon, M. N. Jawaid, J. Bartsch, M. Glatthaar, and S. W. Glunz, "Microstructure analysis of the interface situation and adhesion of thermally formed nickel silicide for plated nickel–copper contacts on silicon solar cells," *Sol. Energy Mater. Sol. Cells*, vol. 117, pp. 209–213, 2013.

[12] R. A. Sinton, A. Cuevas, and M. Stuckings, "Quasi-steady-state photoconductance, a new method for solar cell material and device characterization," in *Conf. Rec. 25th IEEE Photovolt. Spec. Conf.*, Washington, DC, USA, May 1996, pp. 457–460.

[13] H. Nagel, C. Berge, and A. G. Aberle, "Generalized analysis of quasi-steady-state and quasi-transient measurements of carrier lifetimes in semiconductors," *J. Appl. Phys.*, vol. 86, no. 11, pp. 6218–6221, 1999.

[14] R. A. Sinton and A. Cuevas, "Contactless determination of current–voltage characteristics and minority-carrier lifetimes in semiconductors from quasi-steady-state photoconductance data," *Appl. Phys. Lett.*, vol. 69, no. 17, pp. 2510–2512, 1996.

[15] S. Wilking, C. Beckh, S. Ebert, A. Herguth, and G. Hahn, "Influence of bound hydrogen states on BO-regeneration kinetics and consequences for high-speed regeneration processes," *Sol. Energy Mater. Sol. Cells*, vol. 131, pp. 2–8, 2014.

[16] A. Herguth, G. Schubert, M. Kaes, and G. Hahn, "A new approach to prevent the negative impact of the metastable defect in boron doped CZ silicon solar cells," in *Proc. IEEE 4th World Conf. Photovolt. Energy Conf.*, Waikoloa, HI, USA, 2006, pp. 940–943.

[17] A. Herguth, C. Derricks, P. Keller, and B. Terheiden, "Recovery of LeTID by low intensity illumination: Reaction kinetics, completeness and threshold temperature," *Energy Procedia*, vol. 124, pp. 740–744, 2017.

[18] G. Cattaneo *et al.*, "Lamination process and encapsulation materials for glass– PV module design," *Photovolt. Int.*, vol. 27, pp. 1–8, 2015.

[19] Sraisth, "Achieving faster lamination process for crystalline photovoltaic modules by using latest lamination technologies," in *Proc. 36th Eur. Photovolt. Sol. Energy Conf. Exhib.*, 2017, pp. 992–997.

[20] S. Wilking *et al.*, "High speed regeneration of BO-defects: Improving long-term solar cell performance within seconds," in *Proc. 29th Eur. Photovolt. Sol. Energy Conf. Exhib.*, 2014, pp. 366–372.

[21] B. J. Hallam *et al.*, "Advanced hydrogenation of dislocation clusters and boron-oxygen defects in silicon solar cells," *Energy Procedia*, vol. 77, pp. 799–809, 2015.

[22] S. Roder *et al.*, "New approach for a combined process of an ultrafast boron-oxygen defect regeneration and thermal contact treatment of Ni/Cu/Ag plated solar cells," in *Proc. 36th Eur. Photovolt. Sol. Energy Conf. Exhib.*, 2019, pp. 457–563.

[23] T. E. Graedel, "Corrosion mechanisms for silver exposed to the atmosphere," *J. Electrochem. Soc.*, vol. 139, pp. 1963–1970, 1992.

[24] C. E. Sanders, D. Verreault, G. S. Frankel, and H. C. Allen, "The role of sulfur in the atmospheric corrosion of silver," *J. Electrochem. Soc.*, vol. 162, no. 12, pp. C630–C637, 2015.